RSC Advances

PAPER

View Article Online
View Journal | View Issue

Open Access Article. Published on 08 March 2023. Downloaded on 12/4/2025 1:05:34 PM.
This article is licensed under a Creative Commons Attribution-NonCommercial 3.0 Unported Licence.

Check for updates

Cite this: *RSC Adv.*, 2023, **13**, 7645

Novel solid-contact ion-selective electrode based on a polyaniline transducer layer for determination of alcaftadine in biological fluid†

Ola G. Hussein,[a] Dina A. Ahmed,[a] Mohamed Abdelkawy,[b] Mamdouh R. Rezk,[b] Amr M. Mahmoud *[b] and Yasmin Rostom[b]

Received 28th January 2023
Accepted 2nd March 2023

DOI: 10.1039/d3ra00597f

rsc.li/rsc-advances

Fabrication of a novel ion selective electrode for determining alcaftadine was achieved. The glassy carbon electrode (GCE) was utilized as a substrate in fabrication of an electrochemical sensor containing polyaniline (PANI) as an ion-to-electron transducer layer. A PVC polymeric matrix and nitrophenyl-octyl-ether were employed in designing the ion-sensing membrane (ISM). Potential stability was improved and minimization of electrical signal drift was achieved for inhibition of water layer formation at the electrode interface. Potential stability was achieved by inclusion of PANI between the electronic substrate and the ion-sensing membrane. The sensor's performance was evaluated following IUPAC recommendations. The sensor dynamic linear range was from 1.0×10^{-2} to 1.0×10^{-6} mol L^{-1} and it had a 6.3×10^{-7} mol L^{-1} detection limit. The selectivity and capabilities of the formed alcaftadine sensor were tested in the presence of its pharmaceutical formulation excipients as well as its degradation products. Additionally, the sensor was capable of quantifying the studied drug in a rabbit aqueous humor. Method's greenness profile was evaluated by the means of Analytical Greenness (AGREE) metric assessment tool.

1. Introduction

Green Analytical Chemistry (GAC)[1] aims to develop greener analytical methods through minimizing sample preparation steps, safe handling of solvents and reagents, and in addition decreasing energy consumption and waste production. Applying green analytical chemistry, analysts can successfully guarantee reduction of any unwanted complications during analysis while maintaining accuracy, sensitivity, selectivity, and precision of the analytical determination. Potentiometry depends on fabricating ion selective electrodes and is considered to be an environmentally friendly method of analysis.

Ion-selective electrodes (ISEs) have the ability to determine primary ion activity in different matrices[2–6] and are part of the electrochemical sensors family. Being a passive technique, potentiometric measurement is a non-threatening analytical technique which transduces activity of primary ions into electrical potential with no further stimulation. Thanks to their native properties of ease, affordability, smaller size, quickness, and also accuracy, ISEs have been considered for application in a variety of fields such as environmental, biomedical,[7–10] and industrial analysis[11–15] for rapid ion detection.

Recently, potentiometric ion sensors new generation, solid-contact ion-selective electrodes (SC-ISEs) have shown wider implementation range owing to their distinctive advantages such as miniaturization, simple on-site disposable analyzers, fast response, portability, low production cost and ease of usage, as well as low-cost accessible manufacturing techniques. To enhance electrical signal stability of SC-ISEs many ion-to-electron transducers have been introduced such as solid-contact functional materials for instance; conductive polymers (CPs),[16–20] and nanomaterials.[21–27] Addition of these materials improved sensors robustness and reliability, while being calibrated and maintenance free. In comparison to the classical liquid contact, SC-ISEs polymeric membrane achieved the following properties; they become easier in design, more flexible and compatible with modern 3D printing and can be miniaturized.[28] Paper-based electrode fabrication,[29,30] and microfabrication are technologies that produce cost-effective sensor arrays at high throughput.[31–33] Miniature SC-ISEs can be assembled with lab-on-chip devices as well as with other wearable ones[33] because the ease of its production process and high quality. SC-ISEs and wearable technologies mixtures have turn out to be a new promising aspect in research area that allows enormous opportunity for commercialization.[34–37] Moreover, different approaches have been introduced to enhance SC-ISEs in terms of selectivity, biocompatibility, detection limit, sensitivity, anti-biofouling.[38–42] Yet, these SC-

[a]*Pharmaceutical Chemistry Department, Faculty of Pharmacy, Future University in Egypt, Cairo, Egypt*

[b]*Analytical Chemistry Department, Faculty of Pharmacy, Cairo University, Kasr El-Aini Street, Cairo 11562, Egypt. E-mail: amr.bekhet@pharma.cu.edu.eg*

† Electronic supplementary information (ESI) available. See DOI: https://doi.org/10.1039/d3ra00597f

© 2023 The Author(s). Published by the Royal Society of Chemistry

Open Access Article. Published on 08 March 2023. Downloaded on 12/4/2025 1:05:34 PM. This article is licensed under a Creative Commons Attribution-NonCommercial 3.0 Unported Licence.

ISEs encountered several obstacles such as increase potential drift and difficulty of junctioning between electron-conducting solid contact and ion conducting sensing membrane resulted in standard potential (E^0) with time irreproducibility. These obstacles raised between ion selective membrane and solid contact due existence of water layer, it re-equilibrates on every sample composition modification by acting as an electrolyte reservoir and has undesirable action on potential stability and SC-ISEs LOD.[43]

Overcoming the above obstacles, research aimed to embedded interlayer integration on solid contact and liquid membrane. Previously ion to electron transducer layer were applied as carbon nanotubes,[44] lipophilic self-assembled monolayer of thiols[45] and conducting polymers (CP).[16] Applying polyaniline which is considered as conducting polymer in form of hydrophobic redox mediator had significant attention[4,16,17,46,47] and has been focus of research interest as it enhanced the electrochemical sensors performance.

Polymerization of polyaniline can be carried out either electrochemically or chemically. Electrochemical polymerization has many advantages; (1) the process is performed without any free radical initiators, oxidizing agents, or radiation source; (2) polymerization at ambient temperature is accomplished; (3) electrode surface adhered with polymer forms, and ultrathin films; (4) film thickness manipulation and porosity reproduced and achieved by electropolymerization parameters control (potential, current density, and cycles number); and (5) polymerization can be carried out in aqueous acidic solution.

Alcaftadine (ALF); 6,11-dihydro-11-(1-methyl-4-piperidinylidene)-5*H*-imidazo[2,1-*b*]benzazepine-3-carboxaldehyde;[48] Fig. S1,† is a histamine receptor (H1) antagonist[49,50] prescribed to prevent itching related to allergic conjunctivitis. It can act as mast cell stabilizing and immune cell recruitment. Several analytical methods were published in literature for ALF analysis including spectrophotometric,[51,52] high performance liquid chromatographic (HPLC),[53] UPLC-MS,[54] and stability thin layer chromatographic methods.[55,56] As far as the authors know, there hasn't been any electrochemical sensor developed for ALF determination yet.

The objective of the current contribution is to determine ALF in its pure form, dosage form, degradation product, and in spiked rabbit aqueous humor using electrochemically modified glassy carbon electrode (GCE) using PANI. Subsequently ion-selective membrane (ISM) had been drop-casted on GCE modified surface to fabricate (sensor 1); assigned as GCE/PANI/ISM. Furthermore, a comparative study has been performed between sensor 1; GCE/PANI/ISM and a control sensor; sensor 2 consisting of GCE/ISM which was fabricated by omitting the PANI electropolymerization step to examine the impact of PANI on potential stability and sensor performance. The sensors' electrochemical behavior was studied following the IUPAC recommendations and the pH effect was investigated. The impact of PANI inclusion was assessed using water layer test. Finally, analytical greenness (AGREE) assessment tool[1] was applied to determine the influence of the proposed method on the environmental health effects quantitatively and qualitatively.

2. Experimental

2.1. Apparatus

Sigma-Aldrich, Germany supplied us with Ag/AgCl reference electrode double-junction for potentiometric measurements, while pH adjustment is done using a Jenway 3505 pH meter (Staffordshine, UK). Digital ion analyzer (Jenway, United Kingdom) Magnetic stirrer was used. Potentiostat/galvanostat PGSTAT204 (Metrohm Autolab, Netherlands) controlled using Nova 1.11 software was used for electropolymerization and electrochemical.

TLC aluminum plates F_{254} (20×20 cm^2) with 0.25 mm thickness layer, E. Merck (Darmstadt, Germany) was used for oxidative degradation monitoring, and Micro-droppers was used for sample application on plates and spots visualization, for degradation tracing using a 254.0 nm UV lamp.

2.2. Material and reagents

Analytical grading was our choice in all solvents used in procedure, also water was bi distilled. As Sigma-Aldrich, Germany supplied us with aniline, 2-nitrophenyl-octyl-ether (2-NPOE), polyvinyl chloride (PVC), ethanol, potassium tetrakis(4-chlorophenyl)borate (K-TCPB), and tetrahydrofuran (THF), and El Nasr pharmaceutical Co., Cairo, Egypt supplied us with 97% sodium chloride; 98% potassium chloride; 98% magnesium chloride; 98% calcium chloride; 96% sodium hydroxide concentrated hydrochloric acid, concentrated sulphuric acid; 98% sodium dihydrogen phosphate and 30% hydrogen peroxide.

Preparation of phosphate buffer (pH 6.0) was achieved by means of 0.02 mol L^{-1} sodium dihydrogen phosphate and the pH is adjusted using NaOH and animal house of Faculty of Pharmacy, Cairo University supplied us with rabbit aqueous humor obtained from living rabbit.

2.3. Sample

2.3.1. Pure sample. Alcaftadine was purchased from Sigma-Aldrich. According to the reported method[52] its purity was found to be 99.8% ± 0.96.

2.3.2. Market sample. Lastacaft™ ophthalmic solution (Batch Number T1710) was purchased from local market manufactured by Allergan, USA.; each one mL of eye drop contains 2.5 mg alcaftadine.

2.4. Standard solutions

2.4.1. ALF stock standard solution (1.0×10^{-2} mol L^{-1}). ALF stock standard solution was prepared using 25-mL volumetric flask where 0.076 g accurately drug weighed was transferred, then 10.0 mL phosphate buffer, pH 6.0 was used to dissolve it and by using phosphate buffer the volume was completed.

2.4.2. ALF test solutions (1.0×10^{-8} – 1.0×10^{-2} mol L^{-1}). Using suitable dilution from stock standard solution ALF working standard solution was prepared using phosphate buffer pH 6.0.

2.4.3. ALF's oxidative degradation product's standard and working solutions. Oxidative studies was applied by refluxing 25 mg of ALF in 25 mL ethanolic solution of hydrogen peroxide

 © 2023 The Author(s). Published by the Royal Society of Chemistry

Open Access Article. Published on 08 March 2023. Downloaded on 12/4/2025 1:05:34 PM. This article is licensed under a Creative Commons Attribution-NonCommercial 3.0 Unported Licence.

(5%, by volume) and by the use of same solvent volume was completed. Spontaneously oxidative degradation product was obtained, and excess hydrogen peroxide was removed by evaporation. Elucidation was conducted by means of mass and IR spectrometry to identify the degradation product. Oxidative degradation product working solution; 100.0 μg mL^{-1} was prepared using suitable dilution from stock standard solution (1000.0 μg mL^{-1}).

2.5. Electrochemical grafting of polyaniline onto GCE surface

Electropolymerization was performed using potentiostat/galvanostat controlled by Nova 1.11.1 software. GCE was polished mechanically using alumina and rinsed with water, after that the electrochemical polymerization of PANI from 0.1 M aniline as a monomer in 0.1 M H_2SO_4 V s Ag/AgCl as reference electrode and Pt as counter electrode was carried using GCE working electrode. Cyclic voltammetric scan from −0.1 to 1.0 V *vs.* Ag/AgCl reference electrode at 50 mV s^{-1} scan rate for 10 consecutive cycles was carried out for electropolymerization.[57] The modified electrode was characterized by scanning electron microscope and electrochemical impedance spectroscopy in 5 mM $(Fe(CN)_6)^{-4/-3}$ as redox probe in 0.1 M KCl solution.

2.6. Preparation of ion selective membrane and sensor assembly

ALF selective membrane components: total 600 mg were prepared *via* mixing w/w: 33.55% PVC, 65.0% *o*-NPOE and 1.45% K-TCPB dissolved into 6 mL of THF.

The complete sensor (1) GCE/PANI/ISM was formed by ISM drop-casting. The effect of PANI on potential stability was tested to determine potential stability, by fabricating control GCE/ISM sensor (2) lacking PANI layer. At ambient temperature ISEs were kept to dry and vaporize THF after that 1.0×10^{-4} mol L^{-1} ALF used for sensors conditioning.

2.7. Potentiometric measurements and sensors calibration

Double-junction Ag/AgCl reference electrode was used for potentiometric measurements conduction. Making several dilutions using phosphate buffer pH 6.0 from ALF solution were done and electromotive force (*emf*) measurements were acquired to determine the calibrations of ALF. Obtaining calibration curves of interfering substances and ALF's degradation product by means of successive dilutions. Application of separate solution method[58] to determine selectivity coefficients.

2.8. Study of pH effect on sensor performance

The effect of pH (2.5–10.0) on the response of electrode potential was investigated using 1.0×10^{-3} mol L^{-1} and 1.0×10^{-4} mol L^{-1} solutions of ALF. Recording potential obtained at each pH value.

2.9. Selectivity study

In presence of some interfering ions (K^+, Na^+, Ca^{2+}, and Mg^{2+}) and ALF degradation product was measured to study the sensor selectivity and to determine the extent of foreign substance and its effect on the electrode it was calculated by means of the potentiometric selectivity coefficients ($\log K_{AB}$). Following IUPAC guidelines evaluating the selectivity coefficients by the use of separate solutions method (SSM)[59] applying the following equation (eqn (1)),

$$\log K_{AB} = \frac{[E_B - E_A]Z_A F}{2.303\ RT} + \left(1 - \frac{Z_A}{Z_B}\right) \log a_A \qquad (1)$$

where E_A is the potential measured in 1.0×10^{-3} mol L^{-1} solution of interferent ion and E_B is the potential measured in 1.0×10^{-3} mol L^{-1} solution of primary ion solution. Z is the net charge, F is the Faraday constant, R is the universal gas constant, T is the temperature in Kelvins and a_A is activity of interferent ion A.

2.10. Water layer test

PANI based SC-ISEs has improved potentiometric characteristics and short-term stability, while underneath the ion selective membrane an aqueous layer had been formed affecting the long-term stability. The formation of these layer was investigated by Pretsch group[35] introducing potentiometric aqueous layer test. This test was done to detect the potential drift upon the changing happened from an ALF solution (1.0×10^{-3} mol L^{-1}) to the highly concentration interfering ion solution, Antazoline HCl (1.0×10^{-2} mol L^{-1}) and back then to ALF solution (1.0×10^{-3} mol L^{-1}). If the aqueous layer accumulated underneath the ion sensing membrane, potential drift would result from changing the aqueous layer ionic composition.

2.11. Method validation

After optimizing the conditions of ALF potentiometric sensors, the method was further validated according to the ICH guidelines[70] regarding the linearity, accuracy, precision, and limit of detection in order to ensure that the suggested method is appropriate for the required use.

2.11.1. Linearity. Linearity was assessed by analyzing five different ALF concentrations in triplicates. Linear relationship has been established between the measured *emf* response and their corresponding concentrations.

2.11.2. Accuracy. Analytical methodology accuracy is an expression of close agreement between true value and measured value. It is demonstrated as percentage recovery of three determinations of ALF.

2.11.3. Precision. Both interday and intraday precision were examined. The intraday precision ($n = 9$), average of three concentrations repeated three times within the day and the interday precision ($n = 9$), average of three concentrations repeated three times on three consecutive days.

2.11.4. Limit of detection (LOD). The LOD is the lowest concentration detected by the method but not necessarily quantitated as an accurate and precise value. LOD is estimated by extrapolating the lines of the Nernstian (high concentration) and nonresponsive (low concentration) and observing the concentration of the primary ion at the point of intersection of these lines.

Open Access Article. Published on 08 March 2023. Downloaded on 12/4/2025 1:05:34 PM.
This article is licensed under a Creative Commons Attribution-NonCommercial 3.0 Unported Licence.

2.12. Determination of ALF in Lastacaft™ ophthalmic solution

Into 25 mL volumetric flask, Three and half mL of the Lastacaft™ ophthalmic solution were transferred and phosphate buffer solution: pH 6.0 used to complete the volume preparing 1.0×10^{-3} mol L^{-1} of ALF. The proposed sensors: sensor 1 and sensor 2 with conjunction of the double junction Ag/AgCl electrode were used to carry out the potentiometric measurements and potential readings were singly recorded and subsequently the corresponding concentrations were calculated from the corresponding regression equations

2.13. Determination of ALF in spiked rabbit aqueous humour

In two 25 mL volumetric flasks each containing 1 mL aqueous humour, 2.5 mL of 1.0×10^{-2} and 1.0×10^{-3} mol L^{-1} ALF solutions added individually, and the volume completed using phosphate buffer pH 6.0. Separately the potentials were measured, and by computing in the corresponding regression equation ALF concentrations were determined.

3. Results and discussion

Potentiometric determination using ion selective electrode is a very important analytical technique because of its accuracy,

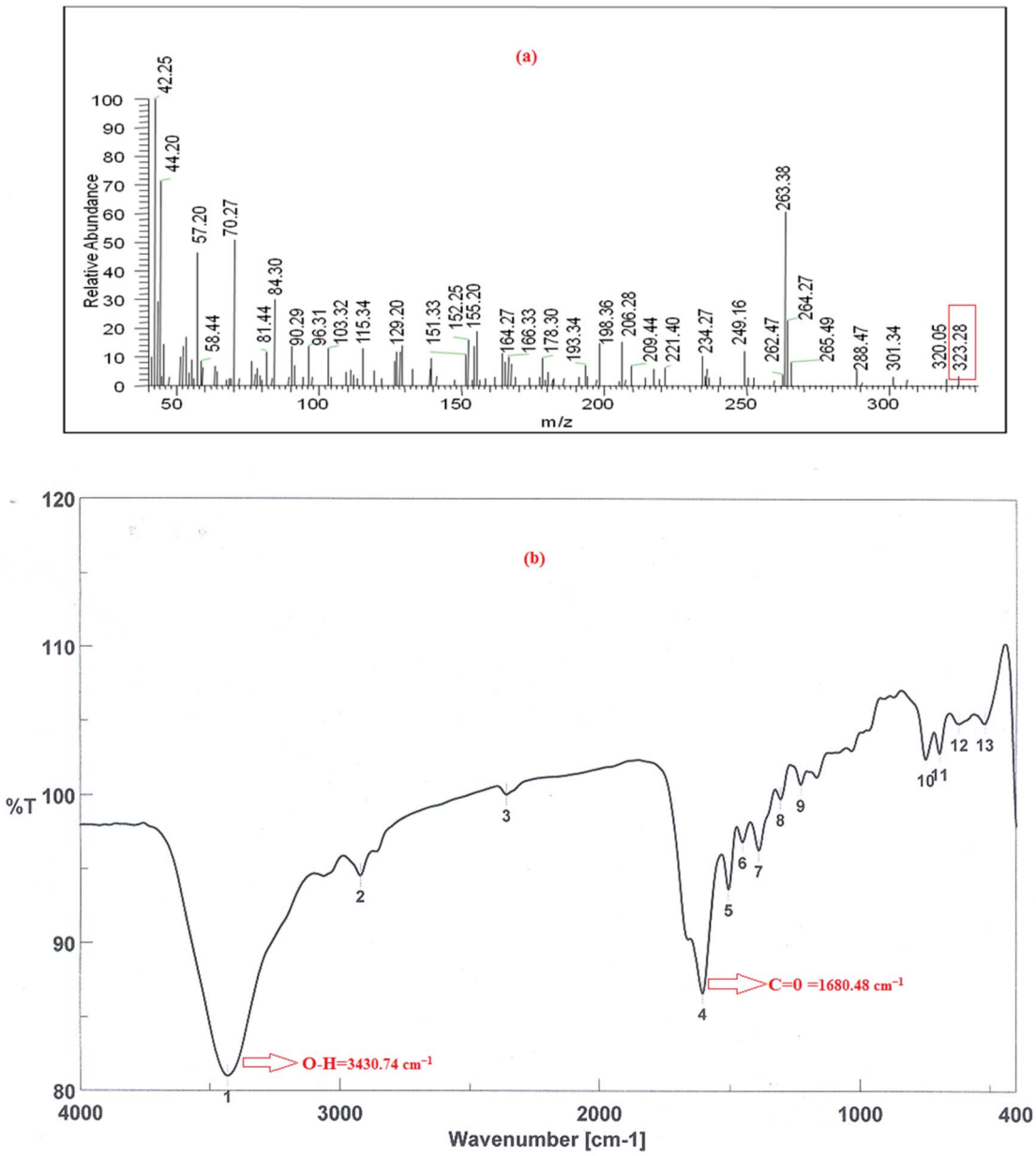

Fig. 1 Mass spectrum (a) and IR spectrum (b) of ALF oxidative degradation product.

 © 2023 The Author(s). Published by the Royal Society of Chemistry

Open Access Article. Published on 08 March 2023. Downloaded on 12/4/2025 1:05:34 PM.
This article is licensed under a Creative Commons Attribution-NonCommercial 3.0 Unported Licence.

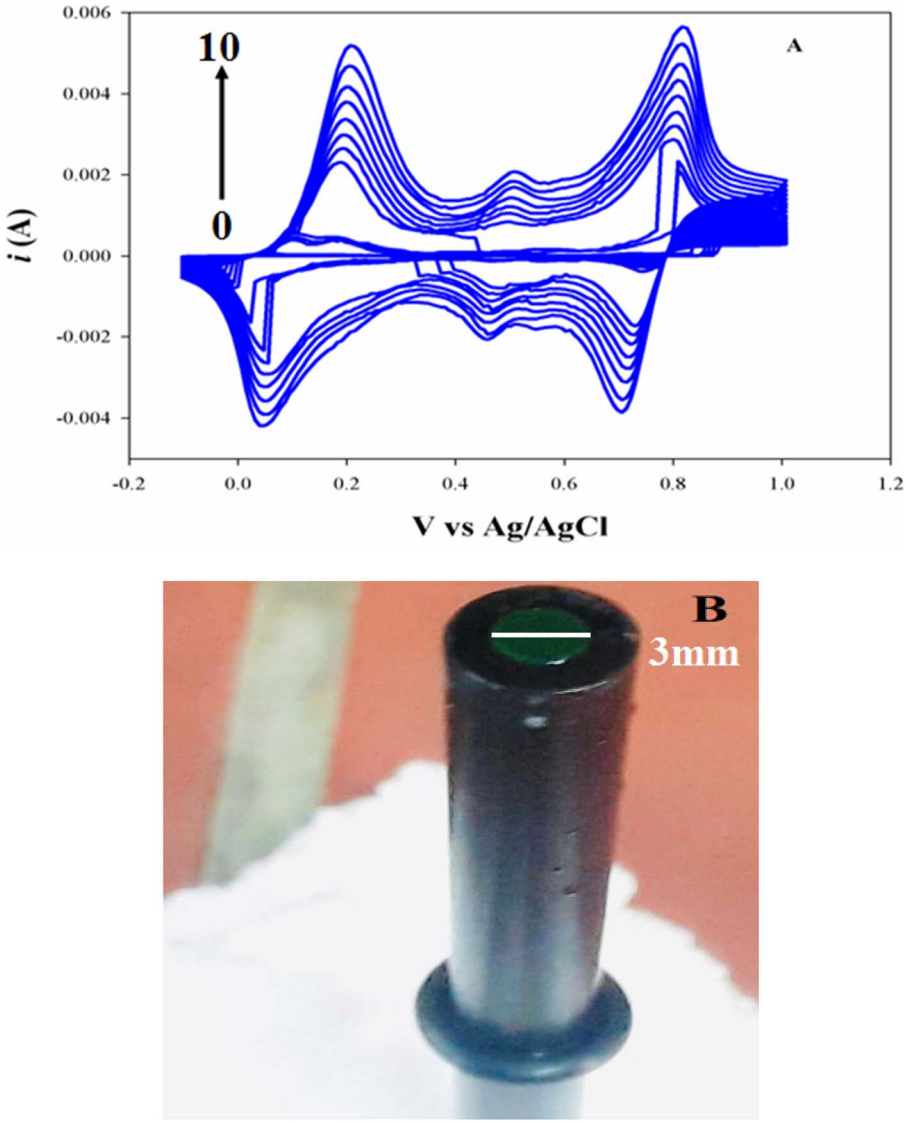

Fig. 2 (A) Electrochemical polymerization of PANI at GCE surface *versus* Ag/AgCl reference electrode using 0.1 M aniline monomer in 0.1 M H_2SO_4 solution by applying potential cycle −0.1 to 1.0 V *vs.* Ag/AgCl at scan rate 50 mV s^{-1} for 10 cycles. (B) Photographic image of GCE/PANI modified electrode.

rapidity, simplicity, eco-friendly beside it's wide application in the analysis of different compounds including pharmaceutical drugs in the dosage forms and biological fluids or the water pollution.[60] Many advantages have arise using ion selective electrodes have over the other analytical methods like spectrophotometric method and HPLC method such as accurate determination of colored, turbid and the viscous samples. In addition to that, it shows fast response to the changes that happen in the concentration, so it can be applied in wide concentration range and still considered as valuable eco-friendly technique.

As a result of the pharmacological importance of the dosage form; our aim is to form stable, environmentally green SC-ISE based on the electropolymerized PANI conducting polymer as ion-to-electron transducer.

3.1. Sensing mechanism of the ion-selective electrode

The part of the electrode that is responsible of the sensing is the membrane that consists of polymer matrix along with the ion exchanger (KTCPB). The polymer matrix is essential to provide a mechanical support for the membrane, while the plasticizer is added to dissolve the ion complex association. The role of the ion exchanger is to bestow the membrane sensitive to the positively charged molecules by exchanging its potassium ions with the positively charged ALF ions, while the ionophore is a neutral molecule that is added to increase in the selectivity of the ion-selective electrode toward the detection of the targeted compounds. This selective response is highly dependent on the molecular recognition where the targeted molecule acts as the guest and the ionophore functions as the host.[61] The molecular recognition leads to a decrease in the free energy of transfer of

Open Access Article. Published on 08 March 2023. Downloaded on 12/4/2025 1:05:34 PM. This article is licensed under a Creative Commons Attribution-NonCommercial 3.0 Unported Licence.

ALF from the sample solution into the polymeric membrane yielding a higher signal of the ion-selective electrode to ALF. The phase boundary potential is an electrical potential generated, at the interface between the membrane of the sensor and the solution of the targeted compound, due to the partitioning of the ionic species resulting in the charge separation at the interface whose magnitude is depending on the concentration of the analyte. This leads to a potential difference between the ion-selective electrode and reference electrode. The potential response is governed by Nernest equation that states that a tenfold change in the concentration will yield in 58.8 mV change in the observed potential. The best results regarding the linear range, slope, and limit of detection were observed in the electrode containing *o*-NPOE as plasticizer.

3.2. ALF's degradation

Different acidic, basic, photolytic, thermal, and oxidative conditions were conducted for stress studies as per ICH guidelines[62] for ALF. It was observed that ALF is stable towards both acidic and basic hydrolysis but susceptible to oxidative degradation only with the production of one degradation product. The suggested degradation pathway of ALF was illustrated in Fig. S2.† Additionally, mass spectrum of ALF's degradate shows a molecular ion peak at 323.28 *m*/*z*; Fig. 1a, and its IR spectrum shows the presence of C=O band of carboxylate group at 1680.48 cm^{-1} with the appearance of a O–H broad band at 3430.74 cm^{-1} Fig. 1b.

3.3. Performance of GCE/PANI/ISM sensor

To fabricate SC-ISEs with repeatable standard potential is still quite challenging.[4] This work represents preliminary experiments to utilize electropolymerized PANI on SC electrodes' detection limit and potential stability. Also, comparing the results of ALF using PANI based SC-ISE (sensor 1) and control SC-ISE (sensor 2).

High potential stability was achieved by a large double layer capacitance that generated by integration of conducting polymer between ion selective membrane and electronically conducting material.[63] The mechanism of transducing PANI can be attributed to faradaic process (Redox capacitance) which involves simultaneous insertion of charge compensatory ions with reversible oxidation of conjugated polymer chains.

The electropolymerization of PANI from 0.1 M aniline as monomer in 0.1 M H_2SO_4 on the surface of GCE is shown in Fig. 2A, during the initial anodic sweeps, spiky anodic peaks around +0.8 V appear in the first three cycles indicating the start of electropolymerization process. Upon subsequent cycles, three anodic peaks are observed with increasing current at every cycle. Similarly, in the cathodic sweep, there are three corresponding broad reduction peaks. Regarding the first peak at +0.2 V, can be attributed to the formation of radical cations (*i.e.* polaronic emeraldine); the second peak around +0.5 V, can be assigned to benzoquinone formation, while, the third peak describes the formation of diradical dications, around at 0.8 V.[64,65] It worth noting that the current increases after each potential cycles indicating that the polyaniline film grows very rapidly as the sweeping proceeds, which reflects the autocatalytic nature of the PANI electropolymerization as described in the literature.[66,67] Fig. 2B presents the photographic image of GCE/PANI modified electrode.

The modified electrode was characterized by scanning electron microscope as shown in Fig. S3,† it shows that the electrode is evenly covered with the PANI polymer. Moreover, the electrochemical impedance spectroscopy (EIS) is a powerful and sensitive tool for studying electrode surfaces. The surface

Table 1 Electrochemical response characteristics of the investigated ALF sensors

	GCE/PANI/ISM	Control GCE/ISM
Parameter	Sensor 1	Sensor 2
Slope (mV per decade)[a]	58.8	57.9
Intercept (mV)[a]	386.8	379.4
Correlation coefficient	0.9999	0.9998
LOD (mol L^{-1})[b]	6.3×10^{-7}	6.3×10^{-7}
Response time (s)	5	20
Working pH range	2.5–7.0	2.5–7.0
Concentration range (mol L^{-1})	$1 \times 10^{-6} - 1 \times 10^{-2}$	$1 \times 10^{-6} - 1 \times 10^{-2}$
Accuracy[a]	100.25	99.65
Precision		
Repeatability[c]	±0.81	±0.97
Intermediate precision[d]	±1.13	±1.25
Stability (days)	30	30

[a] Average of three determinations. [b] Limit of detection (according to IUPAC definition: measured by intersection of the extrapolated arms of non-responsive and Nernstian segments of the calibration). [c] Repeatability: the intraday precision ($n = 9$), average of three concentrations repeated three times within the day. [d] Intermediate precision: the interday precision ($n = 9$), average of three concentrations repeated three times on three consecutive days.

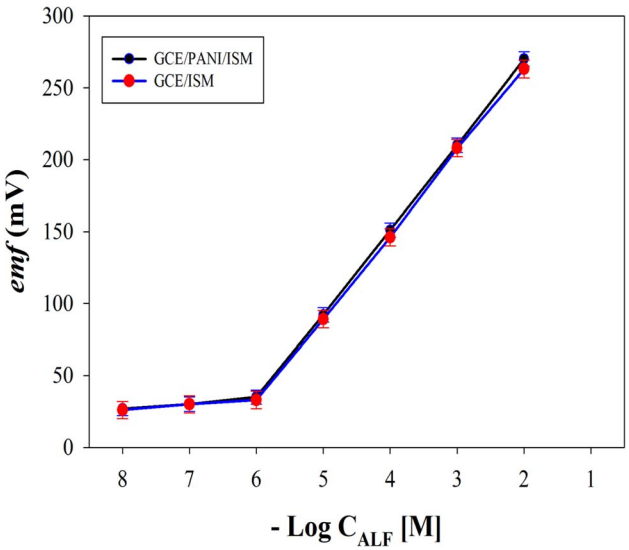

Fig. 3 Profile of the potential in mV *versus* -log molar concentration of ALF in M obtained with sensors 1 and 2.

 © 2023 The Author(s). Published by the Royal Society of Chemistry

Open Access Article. Published on 08 March 2023. Downloaded on 12/4/2025 1:05:34 PM.
This article is licensed under a Creative Commons Attribution-NonCommercial 3.0 Unported Licence.

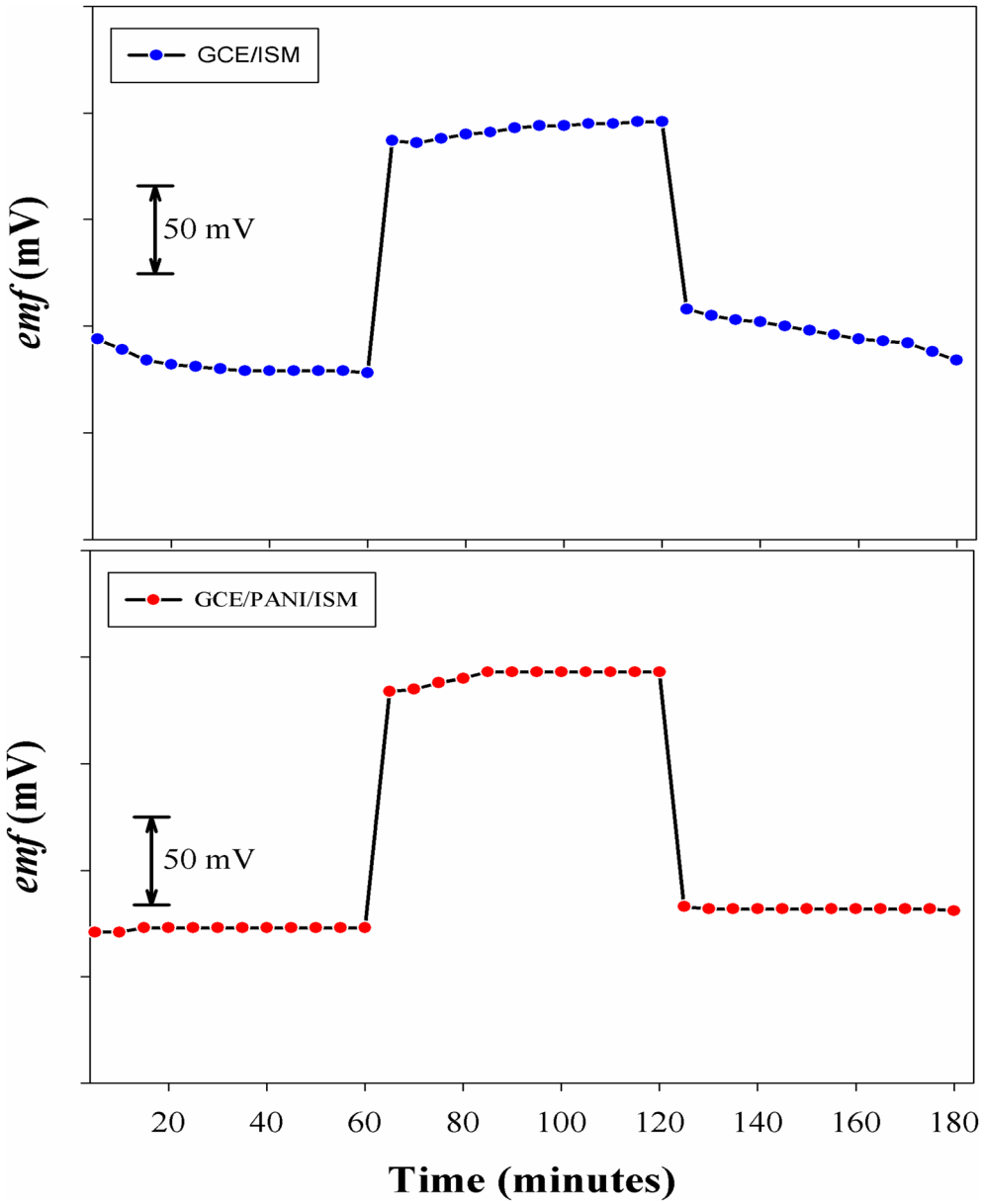

Fig. 4 Water layer test for both GCE/PAN/ISM (sensor 1) and GCE/ISM (sensor 2). The electromotive force (*emf*) was recorded successively in 1.0 $\times 10^{-3}$ mol L^{-1} ALF, 1.0 $\times 10^{-2}$ mol L^{-1} antazoline HCl, and then 1.0 $\times 10^{-3}$ mol L^{-1} ALF using PANI and control SC-ISEs.

characterization of both bare GCE and modified GCE/PANI interfaces was performed by electrochemical impedance spectroscopy. The impedance results were shown as Nyquist plots in ESI Fig. S4.† The results were fitted to Randles circuit using the Nova 1.11.0 software to estimate the solution resistance (R_s), electrode charge transfer resistance (R_{ct}), and constant phase element (CPE). The fitting of the spectra was performed using the equivalent electrical circuit as shown in ESI Fig. S4† inset. For the bare GCE electrode, a small semicircle diameter was found in the Nyquist plot, and the calculated R_{ct} was 245 kΩ, indicating a relatively small electron transfer resistance. While after the modification of electrode with PANI. There is a significant change of charge transfer resistance R_{ct} (580 kΩ). These changes clearly indicate the modification of the GCE electrode with PANI organic film that has less conducting properties than bare GCE. It worth noting that the capacitance increased from 1.35 μF for bare GCE to 35.5 μF at modified GCE/PANI electrode suggesting increase in the electrode surface area.

In accordance with IUPAC standards[68,69] the properties of electrochemical behavior of the two presented sensors are systemically evaluated and illustrated in Table 1. Table 1 represents each sensor validation parameters. Moreover, according IUPAC recommendations[70] LOD was determined and found to be 6.3 $\times 10^{-7}$ mol L^{-1}.

Calibration plots for both sensors with error bars presented in Fig. 3 where the recorded slopes were 58.8 and 57.9 mV per concentration decade for sensors 1 and 2, respectively.

Open Access Article. Published on 08 March 2023. Downloaded on 12/4/2025 1:05:34 PM.
This article is licensed under a Creative Commons Attribution-NonCommercial 3.0 Unported Licence.

Fig. 4 shows PANI minimizing impact on potential drift. Without PANI interlayer (Sensor 2), a drift of 24 mV h^{-1} was noticed in 1.0×10^{-3} mol L^{-1} ALF samples; that was decreased to 0.9 mV h^{-1} with ISEs with PANI interlayer (sensor 1).The formation of water layer between solid contact and membrane phase[46,71,72] decreases potential drift and standard potential reproducibility by time, this problem was evaluated by potentiometric aqueous layer test.

3.4. Potentiometric water layer test

PANI based SC-ISEs, long-term stability is affected by water layer formation beneath the ion-selective membrane. Pretsch group[35] introduced the potentiometric aqueous layer test where the potential drift can be detected upon changing from ALF solution (1.0×10^{-3} mol L^{-1}) to a highly concentrated interfering ion solution, antazoline HCl (1.0×10^{-2} mol L^{-1}) then again to ALF solution (1.0×10^{-3} mol L^{-1}). Fig. 4 reveals water layer formation beneath the membrane during the ion-to-electron transducer layer absence: sensor 2. Where, potential drifts resulted due to change of ionic composition of the water layer by the transmembrane ion fluxes. However, inclusion of PANI in sensor 1 highly stabilized the potential and thus hindered water layer formation at the sensing polymer/electrode interface.

3.5. Dynamic response time

Essential aspect for analytical applications of the ion selective electrodes is the dynamic response time. In this research it was found out that the response time of both sensor 1 and sensor 2 in samples with concentration higher than 1.0×10^{-4} mol L^{-1} were less than ten seconds, while longer time was required to attain stable potential with control SC-ISE.

3.6. pH impact on sensor performance

To be able to study the optimal range from the chemical form aspect of ALF solutions, the potential responses were studied in the pH ranges from 2.5 to 10.0, *emf* 1.0×10^{-3} and 1.0×10^{-4} mol L^{-1} ALF solutions were studied at various pH value and then recorded the obtained potential. Fig. 5 represents that the profile of the potential *versus* pH with error bars for 1.0×10^{-3} and 1.0×10^{-4} mol L^{-1} clarify that the pH ranges from 5.0–7.0 for ALF ($pK_a = 7.16$) is the optimum to obtain a constant potential in which ALF ionizable form was produced and sensed. There is a steady potential decrease probably due to the development of a unionisable form of ALF above this pH range. The medium wasn't acidic sufficient for the piperidine to be dissociated and ionized.

3.7. Sensor selectivity

SSM[59] was applied to calculate the selectivity coefficient, it is considered to be the reliable measurements which reflect the extent the sensor will be affected by the existence of the following substance: excipients, organic and the inorganic related substances. ALF SC-ISE fabricated sensors selectivity was studied in the existence of ALF degradation product. Fig. 6 reveals the separate calibration curves for ALF degradation product and in organic ions (K^+, Na^+, Ca^{2+} and Mg^{2+}). Table 2 show a non-Nernstian response of these ions. This can be attributed to low lipophilic nature of ions which hinder their ion exchange into lipophilic membrane.

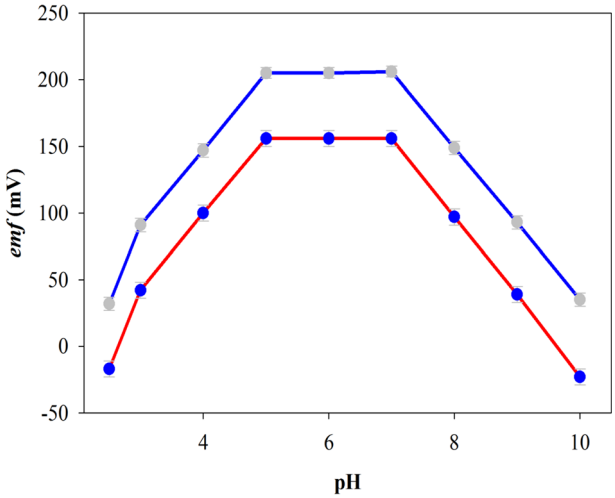

Fig. 5 Effect of pH on the electrical performance of SC-ISEs GCE/PANI/ISM in the range of 2.5–10.0 pH, on both 1.0×10^{-3} and 1.0×10^{-4} mol L^{-1} ALF concentration.

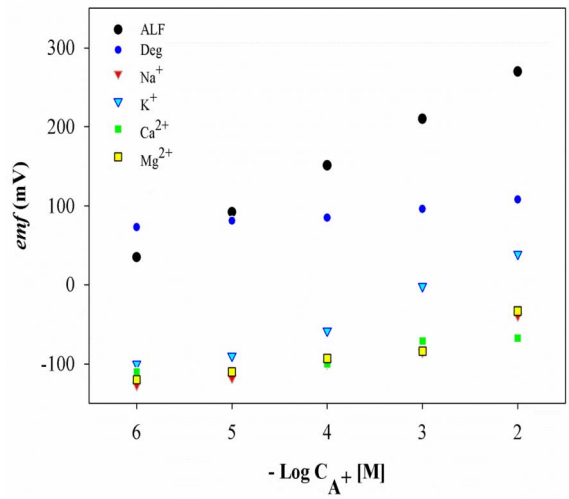

Fig. 6 Calibration curves at GCE/PANI/ISM (sensor 1) obtained for the primary ion; ALF, and potential interferents ions; degradation product, sodium, potassium, calcium and magnesium.

Table 2 Potentiometric selectivity coefficients ($\log K_{AB}$) of the proposed sensor (GCE/PANI/ISM) using the separate solutions method

Interferent, 10^{-3} mol L^{-1}	$\log K_{AB}$
Degrade (degradation product)	−1.94
Na^+	−5.02
K^+	−3.61
Ca^{2+}	−3.28
Mg^{2+}	−3.45

 © 2023 The Author(s). Published by the Royal Society of Chemistry

Open Access Article. Published on 08 March 2023. Downloaded on 12/4/2025 1:05:34 PM.
This article is licensed under a Creative Commons Attribution-NonCommercial 3.0 Unported Licence.

Table 3 Determination of ALF in Lastacaft™ ophthalmic solution by the proposed electrodes and reported method

Dosage form	Recovery (%) ± S.D.[a] of ALF		
	Sensor 1	Sensor 2	Reported method[52]
Lastacaft™ ophthalmic solution, LOT T1710	100.30 ± 0.29	100.79 ± 0.42	100.22 ± 0.36
t-Test (2.770)[b]	0.141	1.785	
F (3.264)[c]	1.54	1.36	

[a] Average of three determinations. [b] The values in parentheses are the corresponding theoretical values for t and F at $p = 0.05$. [c] Zero-order spectrophotometric reported method at λ_{max} 282.0 nm, using methanol as solvent.

3.8. Potentiometric determination of ALF in pharmaceutical formulation

ALF analysis in pharmaceutical formulation (Lastacaft™ ophthalmic solution) was utilized using the fabricated sensors without requiring any sample pre-treatment. The proposed sensors have demonstrated their ability to determine the mentioned drug according to the obtained % recoveries. Percentage recovery results of accurate and precise have proven sensors applicability, Table 3. Results were then compared to those of the reported method[52] to study the validity of the suggested sensors where no statistically significant difference was observed. Moreover, the sample analysis time was short in case of ISE (>1 minute) in comparison to the spectrophotometric reported method in which analysis time is considerably longer.

3.9. Electrochemical measurement of ALF in aqueous humour

ALF concentration in spiked aqueous humour was determined using the suggested sensors. As presented in Table 4 there was broad drug concentration range can be accurately and precisely determined.

3.10. Greenness assessment

In order to eliminate the analytical procedures hazardous chemicals and enhance environmental friendliness method, green analytical chemistry concepts were applied.[1] There are various factors which make the analytical methodologies greenness evaluation very sophisticated like the diversity, the massive number of analytical methods, analytes, sample matrix complexity and the analytical parameters consideration (*e.g.* the precision, accuracy, specificity). Assessment of method greenness *via* applying analytical greenness (AGREE) metric assessment tool depends on evaluating 12 principles of green analytical chemistry; SIGNIFICANCE[1] and are transformed into a unified 0–1 scale then the final score is presented on a pictogram.

Table 4 Determination of ALF in spiked aqueous humour by the proposed sensors

Concentration (mol L^{-1})	Recovery (%) ± S.D.[a]	
	Sensor 1	Sensor 2
1×10^{-3}	98.35 ± 0.27	99.98 ± 0.44
1×10^{-4}	98.88 ± 0.31	100.74 ± 0.38

[a] Average of three determinations.

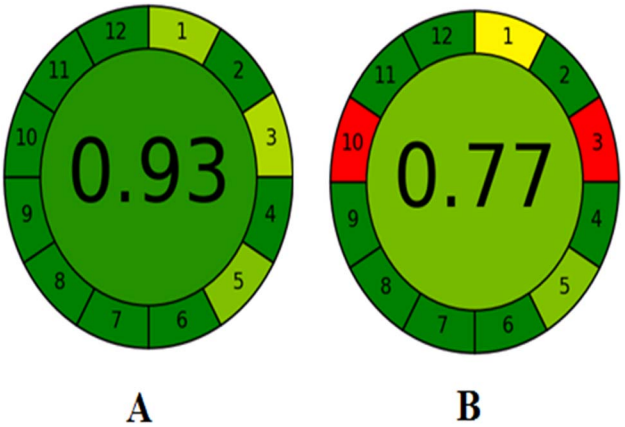

Fig. 7 Greenness assessment of the proposed potentiometric method (A) and the reported spectrophotometric method for ALF (B) *via* analytical greenness (AGREE) metric assessment tool.

Fig. 7 demonstrates AGREE pictograms obtained of the suggested potentiometric method and the reported spectrophotometric one used for ALF analysis. The obtained score of the proposed potentiometric method was 0.93 which was greener than that obtained from the reported method; 0.77. This proves that the proposed method is greener and more environmentally friendly.

4. Conclusion

Nanoscale potentiometery is considered as advancement in ISEs history of which use the nanomaterials to enhance ISEs properties and increase their uses. Adding PANI as interlayer allowed having higher potential stability to the electrical signal (drift of 0.9 mV h^{-1}) in comparison to the PANI free sensor (drift of 24 mV h^{-1}). Beside that PANI based SC-ISEs didn't show any degradation of the electrical response and also have very high stability (from 5.0 to 7.0). Furthermore, an immediate stable potential response was resulted by performing water test which showed water layer absence between the membrane and inner solid contact element. We were successfully able to determine ALF in spiked aqueous humor and in its pharmaceutical formation and in presence of ALF degradation product and interfering ions using the proposed ALF sensor. The current sensor based on GCE is promising to be miniaturized and fabricated on C-SPE or other microfabricated electrodes as a portable point-of-care application. The proposed method greenness profile was done carefully *via* AGREE metric. Eventually, the outstanding stability and worthy piece to piece reproducibility of ALF SC-ISE beside their high greenness

Open Access Article. Published on 08 March 2023. Downloaded on 12/4/2025 1:05:34 PM.
This article is licensed under a Creative Commons Attribution-NonCommercial 3.0 Unported Licence.

profile that makes PANI based solid contact electrodes effective in the usage of routine analysis of ALF in the quality control laboratories.

Ethical statement

All experimental protocols in the current study were approved by the Committee of Safe Handling and Disposal of Chemicals and Biologicals of Research Ethics at the Faculty of Pharmacy, Cairo University (Approved 30/9/2021 with Serial Number AC(3070)). All methods were carried out in accordance with relevant guidelines and regulations. Animal house of Faculty of Pharmacy, Cairo University supplied us with rabbit aqueous humor. All methods are reported in accordance with ARRIVE guidelines.

Author contributions

Ola G. Hussein: conceptualization, methodology, validation, investigation, writing – original draft, visualization. Dina A. Ahmed: conceptualization, methodology, validation, investigation, visualization. Mohamed Abdelkawy: conceptualization, methodology, validation, investigation, visualization. Mamdouh R. Rezk: conceptualization, methodology, validation, investigation, visualization. Amr M. Mahmoud: conceptualization, methodology, validation, investigation, writing – original draft, visualization. Yasmin Rostom: conceptualization, methodology, validation, investigation, visualization.

Conflicts of interest

There are no conflicts to declare.

References

1 F. Pena-Pereira, W. Wojnowski and M. Tobiszewski, *Anal. Chem.*, 2020, **92**, 10076–10082.
2 F. Sallusto, P. Schaerli, P. Loetscher, C. Schaniel, D. Lenig and C. Mackay, *Eur. J. Immunol.*, 1998, **28**, 2760–2769.
3 E. Bakker and M. Telting-Diaz, *Anal. Chem.*, 2002, **74**, 2781–2800.
4 J. Bobacka, A. Ivaska and A. Lewenstam, *Chem. Rev.*, 2008, **108**, 329–351.
5 E. Lindner and B. D. Pendley, *Anal. Chim. Acta*, 2013, **762**, 1–13.
6 M. R. Elghobashy and M. R. Rezk, *Anal. Bioanal. Electrochem.*, 2014, **6**, 461–474.
7 N. F. El Azab, A. M. Mahmoud and Y. A. Trabik, *J. Electroanal. Chem.*, 2022, **918**, 116504.
8 M. R. Rezk, A. S. Fayed, H. M. Marzouk and S. S. Abbas, *J. Solid State Electrochem.*, 2018, **22**, 3351–3361.
9 D. A. Ahmed, M. K. A. El-Rahman, H. M. Lotfy and S. A. Weshahy, *Anal. Bioanal. Electrochem.*, 2020, **12**, 989–1001.
10 D. A. Ahmed, M. K. Abd El-Rahman, H. M. Lotfy and S. A. Weshahy, *J. Electrochem. Soc.*, 2018, **165**, H999.
11 E. Bakker, P. Bühlmann and E. Pretsch, *Chem. Rev.*, 1997, **97**, 3083–3132.
12 A. Lewenstam, *Electroanalysis*, 2014, **26**, 1171–1181.
13 K. Mikhelson and M. Peshkova, 2015.
14 C. Zuliani and D. Diamond, *Electrochim. Acta*, 2012, **84**, 29–34.
15 M. R. Rezk, A. S. Fayed, H. M. Marzouk and S. S. Abbas, *J. Electrochem. Soc.*, 2017, **164**, H628.
16 J. Bobacka, *Electroanalysis*, 2006, **18**, 7–18.
17 J. Bobacka, A. Ivaska and A. Lewenstam, *Electroanalysis*, 2003, **15**, 366–374.
18 A. M. Mahmoud, E. M. Moaaz, M. R. Rezk, E. M. Abdel-Moety and A. S. Fayed, *Electroanalysis*, 2023, **35**, e202200115.
19 S. S. Soliman, A. M. Mahmoud, M. R. Elghobashy, H. E. Zaazaa and G. A. Sedik, *Talanta*, 2023, **254**, 124151.
20 S. A. Hassan, N. W. Nashat, M. R. Elghobashy, S. S. Abbas, A. A. Moustafa and A. M. Mahmoud, *Microchem. J.*, 2022, **178**, 107323.
21 A. Düzgün, G. A. Zelada-Guillén, G. A. Crespo, S. Macho, J. Riu and F. X. Rius, *Anal. Bioanal. Chem.*, 2011, **399**, 171–181.
22 T. Yin and W. Qin, *TrAC, Trends Anal. Chem.*, 2013, **51**, 79–86.
23 R. M. Soliman, Y. Rostom, A. M. Mahmoud, Y. M. Fayez, N. M. Mostafa and H. H. Monir, *Microchem. J.*, 2023, 108381.
24 M. Y. Atta, M. A. Hegazy, A. M. Mahmoud and N. S. Ghoniem, *J. Electrochem. Soc.*, 2022, **169**, 097504.
25 A. M. Mahmoud, M. K. Abd El-Rahman, M. R. Elghobashy and M. R. Rezk, *J. Electroanal. Chem.*, 2015, **755**, 122–126.
26 M. R. Elghobashy, A. M. Mahmoud, M. R. Rezk and M. K. Abd El-Rahman, *J. Electrochem. Soc.*, 2014, **162**, H1.
27 Y. V. M. Reddy, J. H. Shin, J. Hwang, D.-H. Kweon, C.-H. Choi, K. Park, S.-K. Kim, G. Madhavi, H. Yi and J. P. Park, *Biosens. Bioelectron.*, 2022, **214**, 114511.
28 D. L. Glasco, N. H. Ho, A. M. Mamaril and J. G. Bell, *Anal. Chem.*, 2021, **93**, 15826–15831.
29 J. G. Bell, M. P. Mousavi, M. K. Abd El-Rahman, E. K. Tan, S. Homer-Vanniasinkam and G. M. Whitesides, *Biosens. Bioelectron.*, 2019, **126**, 115–121.
30 W.-J. Lan, X. U. Zou, M. M. Hamedi, J. Hu, C. Parolo, E. J. Maxwell, P. Bühlmann and G. M. Whitesides, *Anal. Chem.*, 2014, **86**, 9548–9553.
31 E. Lindner and R. P. Buck, *Anal. Chem.*, 2000, **72**, 336A–345A.
32 H. Y. Y. Nyein, M. Bariya, L. Kivimäki, S. Uusitalo, T. S. Liaw, E. Jansson, C. H. Ahn, J. A. Hangasky, J. Zhao and Y. Lin, *Sci. Adv.*, 2019, **5**, eaaw9906.
33 S. Joo and R. B. Brown, *Chem. Rev.*, 2008, **108**, 638–651.
34 M. Parrilla, M. Cuartero and G. A. Crespo, *TrAC, Trends Anal. Chem.*, 2019, **110**, 303–320.
35 M. Cuartero, M. Parrilla and G. A. Crespo, *Sensors*, 2019, **19**, 363.
36 R. M. Arafa, A. M. Mahmoud, B. M. Eltanany and M. M. Galal, *Electroanalysis*, 2023, **35**, e202200111.
37 N. Magdy, A. E. Sobaih, L. A. Hussein and A. M. Mahmoud, *Electroanalysis*, 2023, **35**, e202200119.
38 Z. Szigeti, T. Vigassy, E. Bakker and E. Pretsch, *Electroanalysis*, 2006, **18**, 1254–1265.

 © 2023 The Author(s). Published by the Royal Society of Chemistry

Open Access Article. Published on 08 March 2023. Downloaded on 12/4/2025 1:05:34 PM.
This article is licensed under a Creative Commons Attribution-NonCommercial 3.0 Unported Licence.

39 M. Guziński, G. Lisak, J. Kupis, A. Jasiński and M. Bocheńska, *Anal. Chim. Acta*, 2013, **791**, 1–12.
40 E. Zdrachek and E. Bakker, *Anal. Chem.*, 2020, **92**, 2926–2930.
41 G. Lisak, T. Arnebrant, A. Lewenstam, J. Bobacka and T. Ruzgas, *Anal. Chem.*, 2016, **88**, 3009–3014.
42 G. Lisak, T. Tamaki and T. Ogawa, *Anal. Chem.*, 2017, **89**, 3943–3951.
43 E. Bakker and E. Pretsch, *TrAC, Trends Anal. Chem.*, 2005, **24**, 199–207.
44 G. A. Crespo, S. Macho, J. Bobacka and F. X. Rius, *Anal. Chem.*, 2009, **81**, 676–681.
45 M. Fibbioli, W. E. Morf, M. Badertscher, N. F. de Rooij and E. Pretsch, *Electroanalysis*, 2000, **12**, 1286–1292.
46 E. Lindner and R. E. Gyurcsányi, *J. Solid State Electrochem.*, 2009, **13**, 51–68.
47 A. Michalska, *Electroanalysis*, 2012, **24**, 1253–1265.
48 R. Namdar and C. Valdez, *Drugs of today*, Barcelona, Spain, 1998, 2011, vol. 47, pp. 883–890.
49 H. Bohets, C. McGowan, G. Mannens, N. Schroeder, K. Edwards-Swanson and A. Shapiro, *J. Ocul. Pharmacol. Ther.*, 2011, **27**, 187–195.
50 J. V. Greiner, K. Edwards-Swanson and A. Ingerman, *Clin. Ophthalmol.*, 2011, **5**, 87.
51 P. R. Mishra, P. Inamdar, P. Jamdar, N. Patel, M. Rohit, D. Satone and D. B. Meshram, *J. Pharma Res.*, 2015, **4**, 9–13.
52 P. R. Mishra, P. Inamdar, P. Jamdar, N. Patel, M. Rohit, D. Satone and D. B. Meshram, *J. Pharma Res.*, 2015, **4**, 14–18.
53 P. Mishra, D. Satone and D. Meshram, *J. Chromatogr. Sep. Tech.*, 2016, **7**, 2.
54 B. B. Chavan, P. D. Kalariya, R. Srinivas and M. K. Talluri, *Chromatographia*, 2018, **81**, 631–638.
55 A. T. Soudi, O. G. Hussein, E. S. Elzanfaly, H. E. Zaazaa and M. Abdelkawy, *Res. J. Pharm. Technol.*, 2020, **13**, 5171–5176.
56 S. A. A. Razeq, S. E. A. Aziz and N. S. Ahmed, *J. Chromatogr. B: Anal. Technol. Biomed. Life Sci.*, 2021, 122804.
57 G. Zotti, S. Cattarin and N. Comisso, *J. Electroanal. Chem. Interfacial Electrochem.*, 1988, **239**, 387–396.
58 E. Bakker, E. Pretsch and P. Bühlmann, *Anal. Chem.*, 2000, **72**, 1127–1133.
59 I. U. o. P. a. A. Chemistry, 2000.
60 V. K Gupta, A. Nayak, S. Agarwal and B. Singhal, *Comb. Chem. High Throughput Screening*, 2011, **14**, 284–302.
61 P. Bühlmann, E. Pretsch and E. Bakker, *Chem. Rev.*, 1998, **98**, 1593–1688.
62 I. Guideline, *Q1A (R2)*, current step, 2003, vol. 4.
63 T. Lindfors, J. Szucs, F. Sundfors and R. E. Gyurcsanyi, *Anal. Chem.*, 2010, **82**, 9425–9432.
64 L. H. Mascaro, A. N. Berton and L. Micaroni, *Int. J. Electrochem.*, 2011, 2011.
65 D. E. Stilwell and S. M. Park, *J. Electrochem. Soc.*, 1988, **135**, 2254.
66 C. H. Yang and T. C. Wen, *J. Electrochem. Soc.*, 1994, **141**, 2624.
67 K. Naoi, K. i. Kawase, M. Mori and M. Komiyama, *J. Electrochem. Soc.*, 1997, **144**, L173.
68 E. Lindner and Y. Umezawa, *Pure Appl. Chem.*, 2008, **80**, 85–104.
69 R. P. Buck and E. Lindner, *Pure Appl. Chem.*, 1994, **66**, 2527–2536.
70 Y. Umezawa, P. Bühlmann, K. Umezawa, K. Tohda and S. Amemiya, *Pure Appl. Chem.*, 2000, **72**(10), 1851–2082.
71 A. Michalska, *Anal. Bioanal. Chem.*, 2006, **384**, 391–406.
72 J.-P. Veder, R. De Marco, G. Clarke, R. Chester, A. Nelson, K. Prince, E. Pretsch and E. Bakker, *Anal. Chem.*, 2008, **80**, 6731–6740.